



HAL
open science

A game of hide and seek between avirulence genes AvrLm4-7 and AvrLm3 in *Leptosphaeria maculans*

Clémence Plissonneau, Guillaume Daverdin, Bénédicte Ollivier, Françoise Blaise, Alexandre A. Degrave, Isabelle Fudal, Thierry Rouxel, Marie-Hélène Balesdent

► To cite this version:

Clémence Plissonneau, Guillaume Daverdin, Bénédicte Ollivier, Françoise Blaise, Alexandre A. Degrave, et al.. A game of hide and seek between avirulence genes AvrLm4-7 and AvrLm3 in *Leptosphaeria maculans*. *New Phytologist*, 2016, 209 (4), pp.1613-1624. 10.1111/nph.13736. hal-02516669

HAL Id: hal-02516669

<https://univ-angers.hal.science/hal-02516669>

Submitted on 24 Apr 2020

HAL is a multi-disciplinary open access archive for the deposit and dissemination of scientific research documents, whether they are published or not. The documents may come from teaching and research institutions in France or abroad, or from public or private research centers.

L'archive ouverte pluridisciplinaire **HAL**, est destinée au dépôt et à la diffusion de documents scientifiques de niveau recherche, publiés ou non, émanant des établissements d'enseignement et de recherche français ou étrangers, des laboratoires publics ou privés.

A game of hide and seek between avirulence genes *AvrLm4-7* and *AvrLm3* in *Leptosphaeria maculans*

Clémence Plissonneau, Guillaume Daverdin, Bénédicte Ollivier, Françoise Blaise, Alexandre Degrave, Isabelle Fudal, Thierry Rouxel and Marie-Hélène Balesdent

INRA, UMR INRA-AgroParisTech 1290-Biogér, Avenue Lucien Brétignières, BP 01, F-78850, Thiverval-Grignon, France

Author for correspondence:

Marie-Hélène Balesdent

Tel: +33 1 30 81 45 73

Email: mhb@versailles.inra.fr

Received: 3 July 2015

Accepted: 27 September 2015

New Phytologist (2016) 209: 1613–1624

doi: 10.1111/nph.13736

Key words: avirulence, *Brassica napus*, durable resistance, interaction, *Leptosphaeria maculans*, next-generation sequencing (NGS), oilseed rape.

Summary

- Extending the durability of plant resistance genes towards fungal pathogens is a major challenge. We identified and investigated the relationship between two avirulence genes of *Leptosphaeria maculans*, *AvrLm3* and *AvrLm4-7*. When an isolate possesses both genes, the *Rlm3*-mediated resistance of oilseed rape (*Brassica napus*) is not expressed due to the presence of *AvrLm4-7* but virulent isolates toward *Rlm7* recover the *AvrLm3* phenotype.
- Combining genetic and genomic approaches (genetic mapping, RNA-seq, BAC (bacterial artificial chromosome) clone sequencing and *de novo* assembly) we cloned *AvrLm3*, a telomeric avirulence gene of *L. maculans*. *AvrLm3* is located in a gap of the *L. maculans* reference genome assembly, is surrounded by repeated elements, encodes for a small secreted cysteine-rich protein and is highly expressed at early infection stages.
- Complementation and silencing assays validated the masking effect of *AvrLm4-7* on *AvrLm3* recognition by *Rlm3* and we showed that the presence of *AvrLm4-7* does not impede *AvrLm3* expression *in planta*. Y2H assays suggest the absence of physical interaction between the two avirulence proteins.
- This unusual interaction is the basis for field experiments aiming to evaluate strategies that increase *Rlm7* durability.

Introduction

During plant colonization, pathogens secrete molecules called effectors that facilitate infection (de Jonge *et al.*, 2011; Koeck *et al.*, 2011). In the course of plant–pathogen co-evolution, some of these effectors, named avirulence (Avr) proteins, have been specifically ‘recognized’ by plant resistance (R) proteins encoded by major resistance genes. The gene-for-gene relationship between an Avr gene and its cognate R gene results in a highly efficient plant response against the pathogen, called Effector-Triggered-Immunity (ETI). In recent years, many Avr/R interactions have been described in a variety of plant–pathogen interactions including plant–bacteria, –oomycetes, –fungi or –nematodes (Catanzariti & Jones, 2010; Wu *et al.*, 2014). Breeding cultivars carrying major resistance genes against pathogens is a common and powerful tool to control disease. However, the massive deployment of a single source of resistance in agronomical practice exerts a strong selection pressure against avirulent pathogens and populations can evolve quickly from avirulence to virulence (McDonald & Linde, 2002).

Leptosphaeria maculans is a Dothideomycete responsible for phoma stem canker, a damaging disease in oilseed rape (*Brassica napus*). Breeding for resistance is the most effective and environmental friendly way to control the disease (Delourme *et al.*, 2006). However, major-gene resistance may be short-lived in

agronomical practice due to the extremely high evolutionary potential of *L. maculans* (Daverdin *et al.*, 2012). In addition the number of efficient qualitative resistance sources is limited in *B. napus* (Balesdent *et al.*, 2006). Fourteen avirulence (*AvrLm*) genes have been identified in *L. maculans*, and six have been cloned: *AvrLm1*, *AvrLm2*, *AvrLm4-7*, *AvrLm6*, *AvrLm11* and *AvrLmJ1* (Gout *et al.*, 2006; Fudal *et al.*, 2007; Parlange *et al.*, 2009; Balesdent *et al.*, 2013; Ghanbarnia *et al.*, 2014; Van de Wouw *et al.*, 2014). All of them encode for small cysteine-rich (except for *AvrLm1*) secreted proteins and are highly expressed at early infection stages. The sequencing of *L. maculans* genome revealed its massive invasion by transposable elements (TEs), which represent *c.* 30% of the genome (Rouxel *et al.*, 2011). In the genome, TEs are clustered and inactivated by repeat induced point mutations (RIP), a premeiotic mechanism specific to fungi (Galagan & Selker, 2004). The RIP mechanism is responsible for the isochore structure of the *L. maculans* genome: GC-isochores display an equilibrated GC (guanine and cytosine) content and contain 95% of the predicted genes, whereas AT (adenine and thymine)-rich isochores are composed of a mosaic of truncated and RIP-degenerated TEs and contain very few genes. However, they contain all currently cloned avirulence genes (Rouxel *et al.*, 2011). Eight of the *L. maculans* *AvrLm* genes are genetically clustered in two distinct regions. The first one contains *AvrLm1*, *AvrLm2*, *AvrLm6*, along with *LmCys2*, which encodes a

candidate effector protein with similar characteristics to those encoded by *AvrLm* genes (Fudal *et al.*, 2007). The second cluster contains *AvrLm3*, *AvrLm4*, *AvrLm7*, *AvrLm9* and *AvrLepR1* (Balesdent *et al.*, 2002, 2005; Ghanbarnia *et al.*, 2012). These clusters can represent hundreds of kbs due to the lack of meiotic recombination in such regions (Rouxel *et al.*, 2011).

Following the cloning of *AvrLm7*, it has been demonstrated that *AvrLm4* and *AvrLm7* are two distinct alleles of a single gene, renamed *AvrLm4-7*. A single base mutation, leading to the change of a glycine to an arginine residue in the avirulence protein, is responsible for the breakdown of *Rlm4* resistance whereas *Rlm7* resistance is unaltered (Parlange *et al.*, 2009). A large-scale survey performed in France in 2000–2001 showed that >99.5% of isolates were avirulent towards *Rlm7* (Balesdent *et al.*, 2006). Only one isolate out of the 1797 sampled was virulent towards *Rlm7*. This isolate showed an avirulent phenotype towards *Rlm3*, whereas this phenotype was extremely rare (<0.1%) at the national scale. Surveys of worldwide populations of *L. maculans*, for example in central Canada, indicated higher frequencies of virulent isolates towards *Rlm7* at some locations. A retrospective analysis of 909 American isolates indicated that >95% of the isolates are either virulent towards *Rlm7* and avirulent towards *Rlm3*, or avirulent towards *Rlm7* and virulent towards *Rlm3* (Dilmaghani *et al.*, 2009). These data, the absence of European field isolates avirulent towards both *Rlm3* and *Rlm7*, and the lack of recombination between *AvrLm3* and *AvrLm4-7* (Balesdent *et al.*, 2002) have questioned whether *AvrLm3* could be a novel allele of *AvrLm4-7*.

In this paper, we report on an unusual gene-for-gene interaction involving the avirulence genes *AvrLm3* and *AvrLm4-7*. We mapped and cloned *AvrLm3*, a novel avirulence gene of *L. maculans* distinct from *AvrLm4-7*. *AvrLm3* is located in a telomeric genomic region, genetically linked to the avirulence gene *AvrLm4-7* and is absent from the reference sequence genome assembly. The presence of a functional allele of *AvrLm4-7* suppresses the *Rlm3*-mediated recognition, in spite of the presence and unaltered expression of *AvrLm3* in *L. maculans* isolates.

Materials and Methods

Terminology

A specific terminology is employed hereafter to facilitate the distinction between isolate interaction phenotypes and genotypes. Considering the interaction between the avirulence gene *AvrLmi* and the resistant gene *Rlmi*, the phenotype of an isolate is termed 'Ai' or 'ai', where 'Ai' corresponds to an avirulent phenotype and 'ai' to a virulent phenotype. The genotype of an isolate with an avirulent allele of an avirulence gene 'i' is written *AvrLmi*, whereas *avrLmi* is assigned to isolates harbouring a virulent allele, whatever the molecular event.

Leptosphaeria maculans (Desm.) Ces. & de Not isolates

The isolate collection from Daverdin *et al.* (2012) originated from an oilseed rape experimental field located in Grignon

(France) where one cultivar harbouring the resistance gene *Rlm7* (Exagone) and one without *Rlm7* (Campala) were grown. *Leptosphaeria maculans* isolates were sampled during three continuous years (2006–2008) on both cultivars. This collection has been phenotyped for virulence towards *Rlm4* and *Rlm7* and the mutational events generating virulence at the *AvrLm7* locus have been determined (Daverdin *et al.*, 2012). From this collection, 1524 isolates (732 A7 and 792 a7) were phenotyped for their virulence towards *Rlm3*. Two A3a7 isolates from this collection (G06-E101 and G06-E107) that were collected from leaf lesions in 2006 on cv Exagone (*Rlm7*) were used in complementation experiments and for *in vitro* crosses. These isolates display two different inactivating mutations in the *AvrLm4-7* gene sequence (Daverdin *et al.*, 2012). Both mutation events introduce premature stop codons in the gene sequence. The reference sequenced isolate v23.1.3 ('JN3', a3A7), from which *AvrLm4-7* was cloned (Parlange *et al.*, 2009), was used for RNA-seq experiments. The a3a7 isolate Nz-T4, in which *AvrLm4-7* is present but displays numerous RIP-induced mutations preventing its PCR amplification (Parlange *et al.*, 2009; accession number KT804641), was used for *in vitro* crosses and for complementation with *AvrLm3*. Isolates G06-E107 (A3a7) and v23.1.2 (a3A7) were used as controls in inoculation tests. All isolates were maintained on V8-agar plates (Ansan-Melayah *et al.*, 1995).

Inoculation tests

All isolates were phenotyped for their virulence towards *Rlm3*, *Rlm4* and *Rlm7* oilseed rape genotypes using a cotyledon-inoculation test (Balesdent *et al.*, 2002). Spore suspensions of each isolate were inoculated on 10–12 plants of each of the *B. napus* cvs or lines Westar (no R gene), 02.23.3.1 (*Rlm7*), Pixel (*Rlm4*) and 03.22.3.1 (*Rlm3*) (Supporting Information Table S1). Symptoms were scored 12–21 d post inoculation (dpi) using a semi-quantitative 1 (avirulent) to 6 (virulent) rating scale in which scores 1–3 represent different levels of resistance (from typical HR to delayed resistance) and 4–6 different levels of susceptibility (mainly evaluated by the intensity of sporulation on lesions) (Balesdent *et al.*, 2005).

In vitro cross

Segregation analysis of *AvrLm3* was performed following an *in vitro* cross between the isolates Nz-T4 (a3a7) and G06-E107 (A3a7) (cross no. 69; Table 1). The cross was performed as described by Gall *et al.* (1994) and Balesdent *et al.* (2001). When pseudothecia had developed and ascospores started to be ejected, mature pseudothecia were stuck upside down on the top of a Petri dish containing 2% water-agar. One to 2 h later, ejection of ascospores was checked using a stereo microscope (Olympus, Rungis, France, SZH10, 70X). Ungerminated, well separated ascospores were randomly selected and moved away from the others, a few millimetres from the ejection spot. After 24 h at room temperature, single germinated ascospores were transferred onto individual V8-agar Petri dishes.

Table 1 Segregation of avirulence of *Leptosphaeria maculans* towards the *Brassica napus* resistance gene *Rlm3* in cross no. 69

	Parental isolate G06-E107	Parental isolate Nz-T4	Phenotypic classes in the progeny			
A3 (phenotype) ^a	A	V	A	A	V	V
A7 (phenotype) ^b	V	V	V	V	V	V
<i>AvrLm7</i> ^c	+	–	+	–	+	–
Number of isolates in each class			56	3	6	57
Total			59		63	

^aA, avirulent phenotype towards *Rlm3*; V, virulent phenotype towards *Rlm3*.

^bV, virulent phenotype towards *Rlm7*.

^c+, the *AvrLm7* gene (virulent allele of G06-E107 towards *Rlm7*) can be amplified by PCR; –, the *AvrLm7* gene cannot be amplified.

DNA manipulation

Genomic DNA was extracted from conidia suspensions using the DNeasy 96 Plant Kit and the Qiagen BioRobot 3000 or DNeasy Plant Mini Kit according to manufacturer's recommendations (Qiagen). Sequencing was performed using a Beckman Coulter CEQ 8000 automated sequencer (Beckman Coulter, Fullerton, CA, USA) according to the manufacturer's instructions or performed by Eurofins Genomics (Eurofins, Ebersberg, Germany).

Design of markers and genetic mapping

The *AvrLm4-7* PCR fragment was used as a marker in cross no. 69 (Table S2). From the molecular markers used by Parlange *et al.* (2009) for *AvrLm4-7* map-based cloning, one minisatellite (*MinLm9*), physically close to *AvrLm4-7*, and three Cleaved Amplified Polymorphic Sequence (CAPS) markers were found to be polymorphic in cross no. 69 (Fig. 1). CAPS fragments (Table S2) were amplified and the PCR products were digested with *Ava*II, *Dde*I and *Bgl*II for markers 46F10_R, 133E3_R and 124F12_F, respectively. Five additional minisatellite markers were designed using the FONZIE pipeline (Bally *et al.*, 2010), one of them, Min12-96, being polymorphic in cross no. 69. Nineteen single-locus PCR markers spanning two truncated copies of degenerated transposons were generated as described by Gout *et al.* (2006) and using the annotation of repeated elements described in Rouxel *et al.* (2011) (Fig. 1; Table S2). All primers were generated using PRIMER3 (Rozen & Skaletsky, 2000). Linkage analyses among loci were performed using the MapMaker/EXP version 3.0b software (available online; Whitehead/MIT Center for Genome Research, Cambridge, MA, USA) with a logarithm of odds (LOD) score of 3.0 and a maximum recombination frequency of 30 cM.

HRM experiments and analyses

High Resolution Melting (HRM) was performed to analyse polymorphic SNPs in cross no. 69 or expression levels in transformed isolates. The HRM mix was composed of 2 µl of DNA or cDNA

template (i.e. 20 ng of DNA or cDNA), 4 µl of each primer (2 µM, Table S2) and 10 µl of SsoFast™ EvaGreen® Supermix (Bio-Rad). PCR amplification was done with a Bio-Rad CFX96 Touch Real-Time PCR Detection System according to the manufacturer's instructions: an initial denaturation step at 98°C for 2 min, followed by 40 cycles at 98°C for 5 s, 60°C for 5 s and a final melting step from 60°C to 95°C with an increase of 0.2°C every 5 s. HRM curve analysis was performed by collecting data from the melting step and results were analysed with the Bio-Rad Melt Curve Analysis™ Software.

RNA extraction, reverse transcription and qRT-PCR analysis

Total RNA was extracted from mycelium or infected cotyledons of the compatible *B. napus* cv Darmor or Darmor-*bzh* using the TRIzol® Reagent (Invitrogen) according to manufacturer's protocol. Total RNA was treated with DNase I RNase-Free (Thermo Fisher Scientific, Waltham, MA, USA). All samples were adjusted to 3 µg of RNA and single-strand cDNA was generated using oligo-dT primed reverse transcription with PrimerScript Reverse Transcriptase (Clontech, Palo Alto, CA, USA) according to the manufacturer's protocol.

Quantitative RT-PCR was performed using a 7700 real-time PCR equipment (Applied Biosystems, Foster City, CA, USA) and Absolute SYBR Green ROX dUTP Mix (ABgene, Courtaboeuf, France) as described by Fudal *et al.* (2007). For each value measured, two to three technical replicates from two biological replicates were performed. Water and uninfected cotyledons were used as negative controls. All primers used for qRT-PCR are detailed in Table S3. Samples were analysed from a 10-fold dilution of the original RT products as described by Fudal *et al.* (2007). The fluorescence threshold (Ct) value was determined at 0.1 of fluorescence intensity.

In order to evaluate the expression profile of avirulence genes over infection, Ct values were analysed according to the method described by Muller *et al.* (2002). In silencing assays, the residual expression of *AvrLm3* and *AvrLm4-7*, compared to those of the wild-type (WT) isolate, were analysed according to the $2^{-\Delta\Delta Ct}$ method (Livak & Schmittgen, 2001). Fungal actin or β -tubulin were used as a constitutive reference gene and *L. maculans* EF1- α relative expression to actin was used as a supplementary control, to verify that there is no variation in the level of expression of actin between conditions and between biological replicates.

Screening of a bacterial artificial chromosome (BAC) clone library

The v23.1.3 *L. maculans* BAC clone library has been described previously (Attard *et al.*, 2002; Gout *et al.*, 2006) and represents a 16-x genome coverage. The library was PCR-screened using 3D-pools (Gout *et al.*, 2006) with primers used for *AvrLm3* genetic mapping: SC12-14, SC12-16, SC12-19, Min12-96, 86520 and 86530 (Fig. 1). Positive BAC clones were extracted using NucleoBond® Xtra Midi/Maxi (Macherey-Nagel, Düren, Germany) according to manufacturer's recommendations.

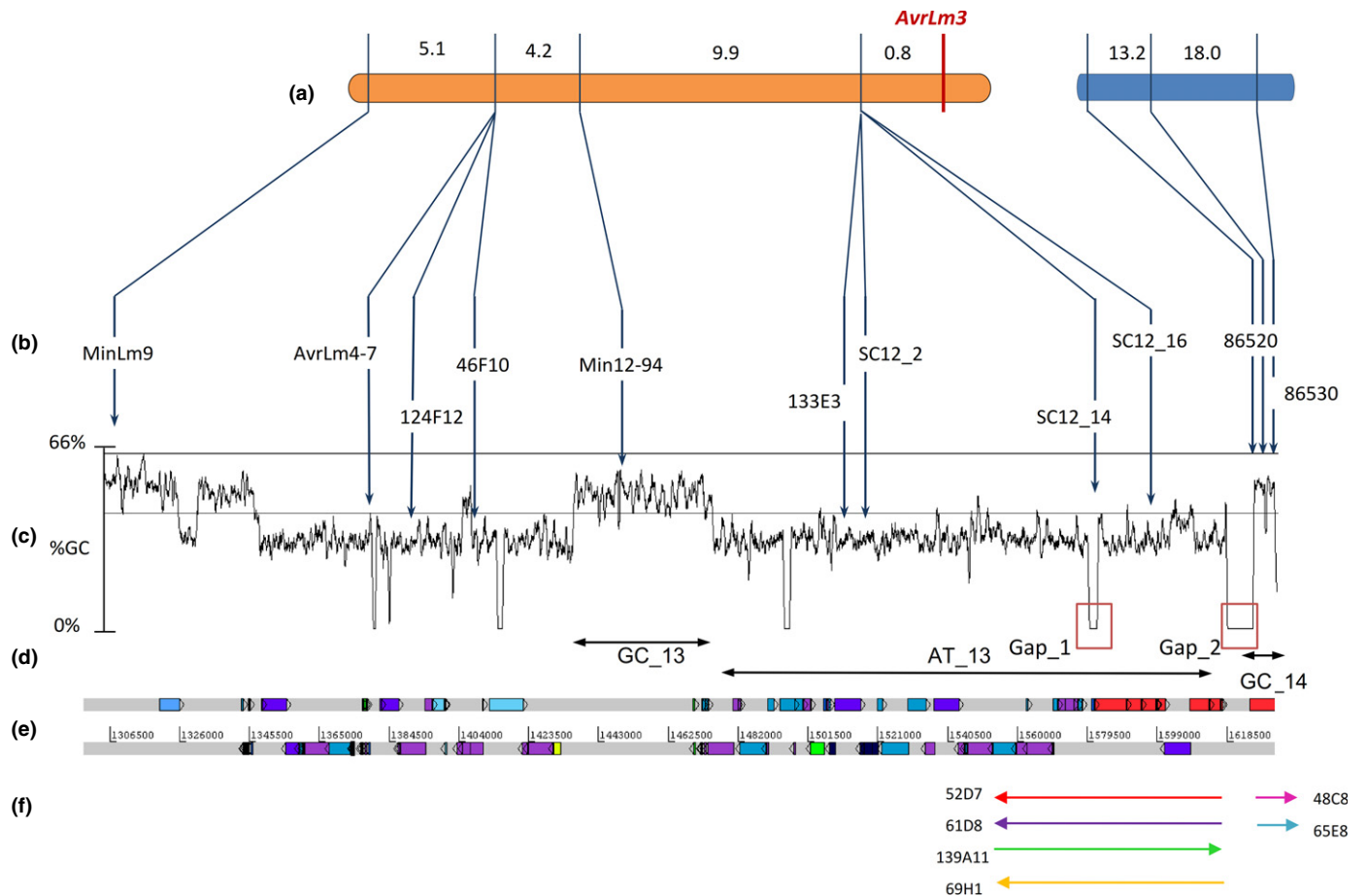


Fig. 1 Genetic and physical maps of the *AvrLm4-7* – *AvrLm3* genomic region of *Leptosphaeria maculans*. (a) Genetic linkage groups of the *AvrLm3*–*AvrLm4-7* region in cross no. 69, with genetic distances in cM. (b) Marker names. The lines connect the genetic location of the markers to their physical position in the corresponding genomic region (3' end of Super-Contig 12 (SC12) of the sequenced isolate v23.1.3). (c) GC content (%) of the sequence along the region (sliding window of 500 bp); the horizontal line indicates the mean GC content (43.74%) of SC12. (d) Position of the last three isochores of SC12, GC_13, AT_13 and GC_14, as defined by their homogeneous GC content, and gaps in the sequence surrounding *AvrLm3* (Gap_1 and Gap_2). (e) Graphical representation of the location of repeated elements as defined by Rouxel *et al.* (2011) on both strands. Each colour corresponds to a given family of repeat. Red boxes correspond to telomere specific repeats (*LmTelo2*). Numbers indicate the scale in bp from the beginning of SC12. (f) Genomic region screened for BAC clones identification and BAC clone names and location. GC, guanine and cytosine; AT, adenine and thymine.

NGS sequencing

BAC clone sequencing (100-bp paired-end reads) was performed using Illumina Mi-Seq technology at Integragen (Evry, France) and generated 1 Gb of sequences. For RNA-seq analysis, cotyledons of the compatible *B. napus* cv Darmor-*bzb* (Chalhoub *et al.*, 2014; Table S1) were inoculated with isolates G06-E107 (A3a7), Nz-T4 (a3a7), v23.1.3 (a3A7), G06-E107 complemented with *AvrLm4-7* (G06-E107 + *AvrLm7*; a3A7), or water (mock condition). Plant tissues around inoculation points were sampled 7 d after inoculation, which is the time when the maximal expression of *AvrLm* genes is usually found (Rouxel *et al.*, 2011), and RNA was extracted. cDNA library construction and sequencing of 50-bp single-reads were performed by the Beijing Genomics Institute (BGI, Shenzhen, China), using Illumina HiSeq2000 technology. A total of 5.2, 4.2, 9.2, 3.9 and 4.1 Gb were obtained for the plant samples inoculated with G06-E107, Nz-T4, v23.1.3, G06-E107 + A7 and mock condition, respectively.

Bioinformatics analysis

The CLC Genomics Workbench v.7.5.1 (Qiagen) was used to analyse NGS data, including *de novo* assembly, gene prediction, RNA-seq mapping and gene annotation.

Fungal transformation

Leptosphaeria maculans transformation was performed using *Agrobacterium tumefaciens* (Gout *et al.*, 2006). Fungal transformants were selected on 50 µg ml⁻¹ nourseothricin (WERNER BioAgents, Jena, Germany). Vectors and isolates used for transformations are listed in Table S4. Two constructs from Parlange *et al.* (2009) were used in complementation experiments. Both constructs are based on the vector pPZPnat1 and differ for the allele of *AvrLm4-7* they carry. The first one termed pPZPnat1-A4A7 carries the v23.1.3 *AvrLm4-7* allele (*AvrLm4-AvrLm7*), whereas pPZPnat1-a4A7 carries the v23.1.2

allele (*avrLm4-AvrLm7*). Vector pPZPnat1-A3 carries a 1357-bp insert containing *AvrLm3* and its promoting and terminating regions, amplified from genomic DNA of G06-E107 with the *AvrLm3*ext-SpeI and *AvrLm3*ext-XhoI primers (Table S3). This insert was ligated in pPZPnat1 previously excised with *SpeI* and *XhoI*. Vector pPZPnat1-sil*AvrLm4-7* and pPZPnat1-sil*AvrLm3* were constructed for RNA-mediated gene silencing of *AvrLm4-7* and *AvrLm3*, using the method described by Fudal *et al.* (2007). Vector pJK11 was used for the construction of inverted repeats of the target genes. The hairpin inverted fragments for each construct were obtained using the primers described in Table S3. Vectors pJK11-*AvrLm4-7* and pJK11-*AvrLm3* were constructed after ligation in pJK11 previously digested by *XmaI* and *BamHI* and *HindIII* and *EcoRI*, respectively. These vectors were incised with *SpeI* and *XhoI* and the fragments containing the hairpin, the *gdpA* promoter and the *trpC* terminator of pJK11 were ligated into *SpeI-XhoI* digested pPZPnat1 to create the final vectors pPZPnat1-sil*AvrLm4-7* and pPZPnat1-sil*AvrLm3*. All plasmids were introduced into *A. tumefaciens* C58-pGV2260 by electroporation at 2.5 kV, 200 Ohms and 25 μ F.

Yeast two-hybrid assay

Yeast two-hybrid (Y2H) assay was performed using the Matchmaker™ Gold Yeast Two-Hybrid System kit (Clontech, takara, Shiga, Japan) according to manufacturer's recommendations. The genes *AvrLm3* and *AvrLm4-7* were amplified from cDNA of isolate v23.1.3 (Table S3) and introduced into vectors pGBKT7 and pGADT7. Vectors pGBKT7 (prey protein) and pGADT7 (bait protein) were introduced into *Saccharomyces cerevisiae* strains Y2HGold and Y187, respectively. Crosses between Y187-*AvrLm3* and Y2HGold-*AvrLm7*, or between Y187-*AvrLm4-7* and Y2HGold-*AvrLm3*, were performed by co-culture of both strains for 24 h in 2 \times YPDA broth at 30°C and 200 rpm. Serial dilutions (10^{-1} , 10^{-2} , 10^{-3} and 10^{-4}) were spotted on selective media and incubated for 3–5 d at 30°C. For all Y2H experiments, a positive control (the diploid strain Y187-T \times Y2Hgold-P53) and a negative control (the diploid strain Y187-T \times Y2Hgold-Lam) were included according to manufacturer's recommendations. The strain Y2H-Gold-*AvrLm4-7* was also used for Y2H screen to identify *AvrLm4-7* putative interactors in a cDNA library from a pool of cotyledons of line 02.23.2.1 (*Rlm7*) inoculated with the isolate 19.4.24 (A3a7) and harvested at 3 dpi, 7 dpi and 14 dpi.

Results

AvrLm4-7 suppresses the expression of the *AvrLm3* phenotype

From 2004 to 2008, a field experiment was conducted in France to monitor the evolution of fungal populations towards the newly released *Rlm7* resistance gene when submitted to an increased and constant *Rlm7* pressure (Daverdin *et al.*, 2012). After 4 yr of *Rlm7* selection pressure, the frequency of isolates virulent towards *Rlm7* had reached 36.2%. The mutational events responsible for

virulence were diverse, with a majority of complete deletion of *AvrLm4-7* or inactivating RIP-mutations (Daverdin *et al.*, 2012). Here, a selection of 1524 isolates (734 A7 and 790 a7) from Daverdin *et al.* (2012) was phenotyped for their virulence towards *Rlm3*. All A7 isolates displayed an a3 phenotype, whereas 785 of the 790 a7 isolates displayed an A3 phenotype, and 5 were virulent towards both *Rlm3* and *Rlm7*. These results led us to hypothesize that the avirulence gene *AvrLm3*, which was regarded as absent in French field populations (Balesdent *et al.*, 2006), is present in most isolates, but that their A3 phenotype is 'hidden' by the presence of a functional allele of *AvrLm4-7*. When *AvrLm4-7* is deleted or inactivated, the gene-for-gene interaction between *AvrLm3* and *Rlm3* is restored.

In order to validate the hypothesis of a negative interaction between the two avirulence phenotypes, two A3a7 isolates with an inactivated *AvrLm4-7* gene, G06-E101 and G06-E107, were complemented with two different alleles of *AvrLm4-7*. All transformants were still virulent on the susceptible cv Westar (Fig. 2e, f). Complementation with a functional *AvrLm4-7* allele restored the avirulent phenotype towards *Rlm7* for all isolates but two (Figs 2a,b, S1). In the two transformants in which the avirulence phenotype towards *Rlm7* was not restored, the absence of integration of the *AvrLm4-7* copy was checked by PCR of the nourseothricin resistance marker gene (Table S3). Inoculation of the transformants on *Rlm3* plants showed that the presence of a functional copy of *AvrLm4-7*, regardless of its allele, resulted in the loss of expression of the *AvrLm3* phenotype (Fig. 2c,d). As a complementary approach, *AvrLm4-7* was silenced in the reference a3A7 isolate v23.1.3. The avirulence towards *Rlm3* was restored whenever the expression level of *AvrLm4-7* was < 10% of that of the WT isolate (Fig. S2). These results confirmed the hypothesis that *AvrLm3* phenotype is hidden by the presence of *AvrLm4-7* and suggested that *AvrLm3* is present in the genome of the sequenced v23.1.3 isolate.

Genetic mapping of the *AvrLm3* locus

The *in vitro* cross no. 69 was performed between isolates G06-E107 (A3a7; for which the inactivated allele can still be amplified by PCR) and Nz-T4 (a3a7; for which no PCR amplification of *AvrLm4-7* can be obtained). One hundred and twenty-two progeny were phenotyped for their avirulence towards *Rlm3* and the 63:59 virulent:avirulent segregation ratio confirmed that the *AvrLm3* phenotype is under a single gene control ($\chi^2 = 0.131$, *P*-value = 0.717) (Table 1). PCR analysis of the *AvrLm4-7* locus segregation revealed that recombination occurred between *AvrLm4-7* and *AvrLm3*, proving that *AvrLm3* and *AvrLm4-7* are not allelic (Table 1). The low number of recombinant isolates compared to parental types confirmed the tight genetic linkage between *AvrLm3* and *AvrLm4-7* loci.

Progeny of cross no. 69 were used to initiate a map-based cloning of *AvrLm3*. Twelve polymorphic markers were identified in the 5' end of the SuperContig (SC) 12 of the *L. maculans* assembly where *AvrLm4-7* is located. They were used to construct a genetic map of the region, composed of two linkage groups (LG) (Fig. 1a). One LG contained the three markers

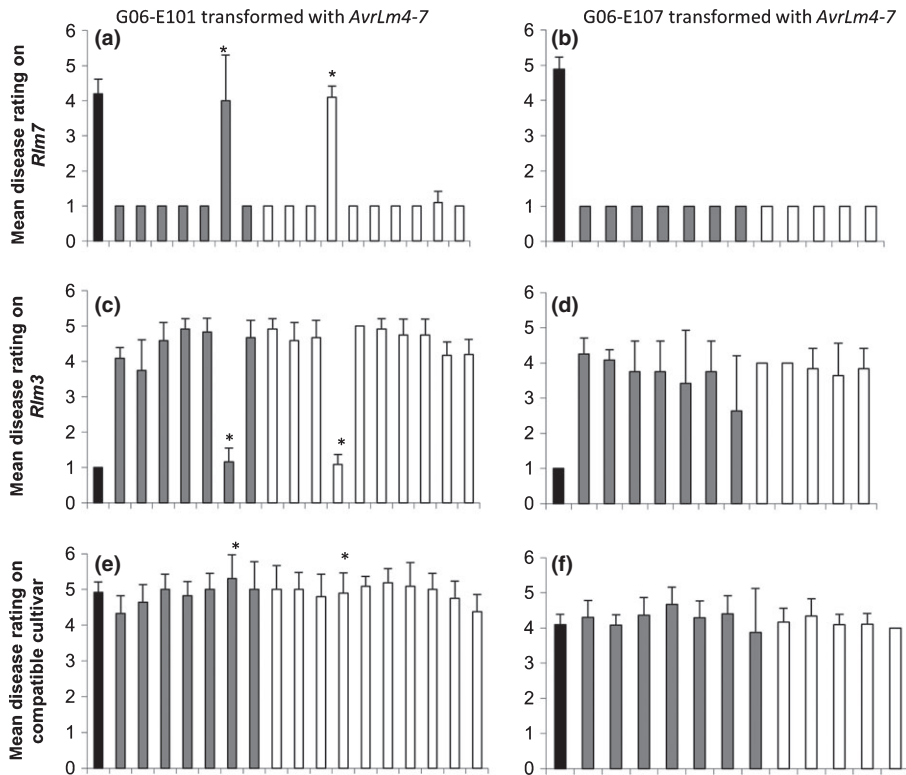


Fig. 2 Interaction phenotypes between *Brassica napus* lines and *Leptosphaeria maculans* isolates complemented with the a4A7 and A4A7 alleles of the *AvrLm4-7* gene. Each vertical bar corresponds to one wild-type (black bars) or transformed (grey or white bars) isolate. Two field A3a7 isolates, that are displaying a virulent phenotype towards *Rlm7* and an avirulent phenotype towards *Rlm3* (G06-E101 (a, c and e) and G06-E107 (b, d and f), black bars) were transformed with the a4A7 (grey bars) or A4A7 (white bars) alleles of the *AvrLm4-7* gene. Isolates were inoculated on *Brassica napus* lines containing *Rlm7* (a, b), *Rlm3* (c, d) or on the compatible cultivar Westar (e, f). The symptoms were assessed 14 d post inoculation (dpi) on a 1–6 scale: 1–3, resistance responses of the plant; 4–6, susceptibility to pathogen. The asterisks indicate false positive transformants that did not integrate the *AvrLm4-7* copy. The experiment was repeated twice and error bars represent + SD.

(Min12_96, 86520 and 86530) located in the last GC-isochore of SC12, GC_14 (Fig. 1). This LG covered a genetic distance of 31.2 cM for a physical distance of 50 kb. The second LG contained *AvrLm3* along with nine molecular markers and marker order in this LG was consistent with the physical map deduced from the genome assembly of the reference v23.1.3 isolate (Rouxel *et al.*, 2011) (Fig. 1a,c). Three of these markers were designed at the junction of two repetitive elements (SC12_2, SC12_14 and SC12_16; Fig. 1) in the last AT-isochore of SC12. Genetic mapping indicated that *AvrLm3* is located in the 3' region of AT_13 (Fig. 1). AT_13, sized 162 kb, encompassed the typical mosaics of RIP degenerated and truncated transposable elements making up AT-isochores in *L. maculans*. Markers SC12_2, SC12_14 and SC12_16 co-segregated but covered a physical distance of 125 kb, in which no ORF was predicted. RNA-seq reads generated from infected cotyledons were mapped on the genome but no additional unpredicted ORFs could be identified in this region. No additional polymorphic marker could be designed to border the *AvrLm3* genetic interval on its 3' side.

Construction of BAC contigs containing the *AvrLm3* locus and identification of an *AvrLm3* candidate

PCR markers located in AT_13 and GC_14 of SC12 were used to identify BAC clones potentially containing the *AvrLm3* locus. Six BAC clones were identified (Fig. 1f). The clones contained either markers from AT_13 or markers from GC_14. No BAC clone linking the two LG could be identified (Fig. 1f). Sequencing and *de novo* assembly of the BAC clones generated 13 contigs

covering a total size of 160 kb. These contigs are composed mainly of RIP-degenerated retrotransposons RLC_ *Pholy*, RLG_ *Oolly* and RLG_ *Polly*, and the telomere-associated repeat *LmTelo2*. The lack of genetic linkage between the two LGs in the *AvrLm4-7-AvrLm3* region was confirmed, with the absence of overlapping sequence between contigs assembled from the BAC clones from each side of Gap_2 (Fig. 1). The fragmentation of the BAC clone assembly in 13 contigs did not allow us to validate the assembly of isochore AT_13. The BAC clone assembly contained a 2.5-kb sequence absent from the genome assembly of *L. maculans*.

RNA-seq reads from cotyledons infected with isolates displaying, or not, an A3 phenotype (Nz-T4, G06-E107, G06-E107 + *AvrLm4-7*, v23.1.3) were mapped on the 13 contigs and only one expressed gene was identified. This gene is one of the 20 most highly expressed genes of *L. maculans* at early infection stages (Table S5) for all isolates used in RNA-seq experiments, whether expressing an A3 or an a3 interaction phenotype. This gene displayed sequence polymorphism in the a3a7 isolate Nz-T4 compared to other isolates, with eight polymorphic nucleotides, of which five are responsible for nonsynonymous mutations (Fig. 3c; Table S6). This sequence polymorphism was used to map the gene in cross no. 69 using the HRM method (Table S2; Fig. S3a). The candidate gene co-segregated with the *AvrLm3* phenotype in the whole progeny.

The *AvrLm3* candidate gene (accession no. KP939098) is 480 nt long and encodes for a 160 amino acids, cystein-rich (ten cysteins in the mature protein) secreted protein (SIGNALP 4.1; Petersen *et al.*, 2011) (Fig. 3b). The 91-bp 3' UTR, 164-bp 5' UTR and the intron of the candidate gene were annotated using

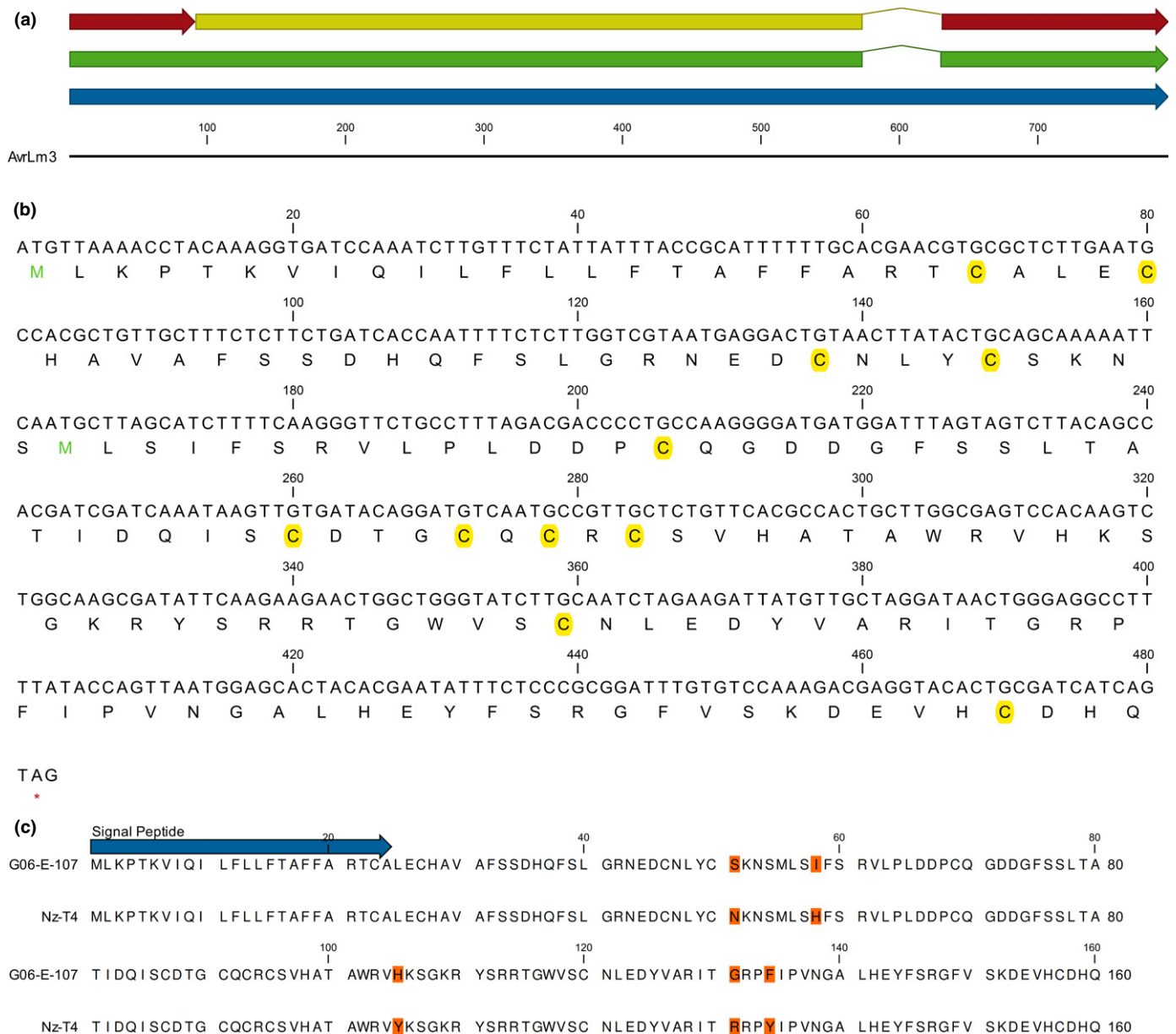


Fig. 3 *AvrLm3* annotation, sequence and polymorphism. (a) The gene, mRNA, coding DNA sequence (CDS) and untranslated region (UTR) are shown in blue, green, yellow and red, respectively. (b) Nucleotide sequence of *AvrLm3* and corresponding amino acids. The signal peptide is marked by the blue line and cysteine residues are highlighted in yellow. (c) The five polymorphic amino acids between the virulent isolate Nz-T4 and the avirulent isolate G06-E107 are highlighted in orange.

the mapping of RNA-seq reads. The 56-bp intron is bordered by the TA and G bases of the STOP codon (Fig. 3a). *AvrLm3* showed no homology with other proteins, except a 29% identity with the newly characterized *L. maculans* avirulence protein *AvrLmJ1* (Van de Wouw *et al.*, 2014), with a conservation of the position of six cysteine residues (Fig. S4).

Functional validation of the *AvrLm3* candidate

The *AvrLm3* candidate gene and its promoting and terminating region (1357 bp) were cloned and transformed into Nz-T4. Ten transformants were recovered and phenotyped on an *Rlm3* genotype or on the susceptible cultivar Pixel. All transformants

showed an unaltered virulent phenotype on Pixel (Fig. 4). Avirulence towards *Rlm3* was restored in seven transformants, whereas three transformants induced variable plant responses with only part of the plants expressing a resistance response (Fig. 4). Because the a3a7 Nz-T4 isolate possesses a virulent allele of the *AvrLm3* candidate gene which is expressed *in planta*, we checked the expression level of each allele (i.e. the virulent and the avirulent one) in all transformants. This was done by HRM analysis on cDNA of the plant–fungus interaction 7 dpi with compatible cv Darmor (Fig. S3b). Both alleles of *AvrLm3* were expressed in all transformants, as revealed by the intermediate melting curves obtained with complemented isolates compared to each WT isolate (Fig. S3b). For the seven transformants in which avirulence

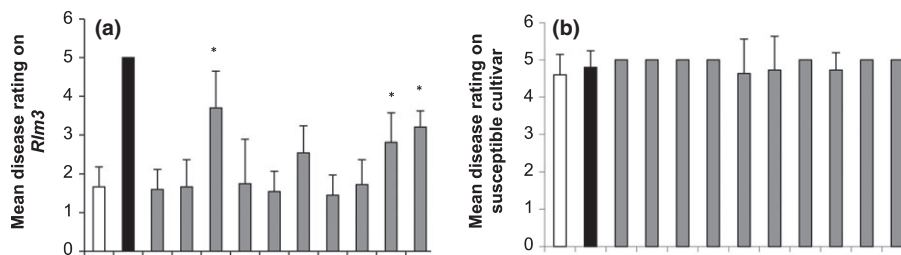


Fig. 4 Interaction phenotypes between *Brassica napus* lines and *Leptosphaeria maculans* a3a7 isolate Nz-T4 complemented with the *AvrLm3* gene. Each vertical bar corresponds to one wild-type (black or white bars) or transformed (grey bars) isolate. The a3a7 isolate Nz-T4 (black bars), possessing a virulent allele of *AvrLm3* was transformed with the avirulent allele of *AvrLm3* (grey bars). G06-E107 was used as a A3a7 control (white bars). Isolates were inoculated on *Brassica napus* lines containing *Rlm3* (a) or the compatible cultivar Pixel (b). The symptoms were assessed 14 d post inoculation (dpi) on a 1–6 scale (1–3, resistance responses of the plant; 4–6, susceptibility to pathogen). The three isolates marked with an asterisk are isolates in which the expression of the avirulent allele of *AvrLm3* is lower than that of the virulent allele and do not fully restore the avirulence phenotype (see Supporting Information Fig. S3). The experiment was repeated twice and error bars represent + SD.

towards *Rlm3* is restored, the intermediate melting curves are clustered together, whereas for the three isolates displaying intermediate phenotypes, the melting curves are grouped in a distinct cluster, closer to the melting curves obtained for the virulent isolate Nz-T4 (Fig. 3b), suggesting a lower expression of the avirulent allele of *AvrLm3* in these transformants, probably insufficient to fully restore the avirulence phenotype (Fig. S3c).

As a complementary approach, the *AvrLm3* candidate gene was silenced in the A3a7 isolate G06-E107. Eight transformed isolates showing different levels of silencing of the *AvrLm3* gene were assessed for pathogenicity towards *Rlm3* and *Rlm7* *B. napus* lines. Silencing levels of *AvrLm3* ranged from 80% to 8% of that of the WT isolate (Fig. S5a). Intermediate levels of silencing led to the development of intermediate resistance phenotypes on *Rlm3*. The two isolates with the lowest level of expression of *AvrLm3* were able to induce susceptibility symptoms on >50% of the inoculated *Rlm3* plants (Fig. S5a). Consistent with the very high level of expression of *AvrLm3* at 7 dpi (Table S5), the level of silencing obtained here was probably insufficient to lead to a

fully virulent phenotype. A similar effect has been previously observed for the *AvrLm6* avirulence gene of *L. maculans* (Fudal *et al.*, 2007).

Both complementation and silencing experiments suggest that the candidate gene encodes for the avirulence protein *AvrLm3*.

AvrLm4-7 does not modify *AvrLm3* expression profile during infection

AvrLm3 shows the same expression kinetics in G06-E107 (A3a7), Nz-T4 (a3a7) and v23.1.3 (a3A7), with low expression during *in vitro* growth and overexpression during early infection stages, especially at 7 dpi (Fig. 5). Compared to that of *AvrLm4-7*, the expression level of *AvrLm3* is 3.4× higher and the overexpression of *AvrLm3* takes place earlier during the infection process (Fig. 5). Although the gene is expressed at a higher level during axenic growth in Nz-T4 compared to G06-E107 or v23.1.3, the expression kinetics of *AvrLm3* is comparable whether the gene encodes for a virulent or an avirulent allele, confirming that the

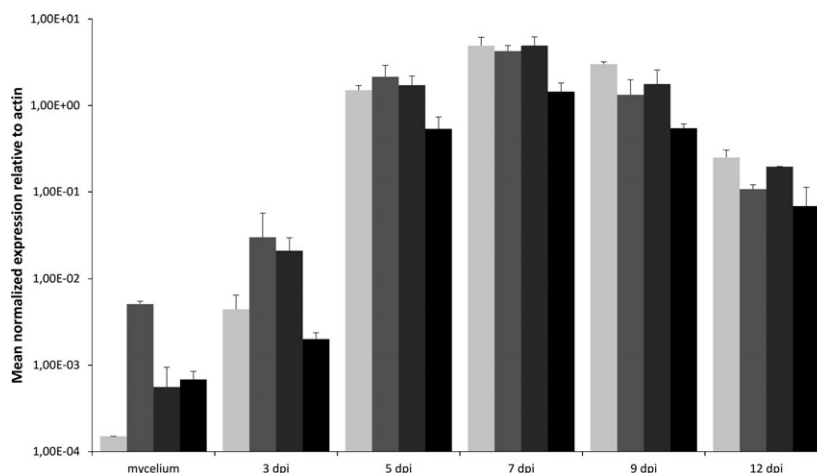


Fig. 5 *AvrLm3* and *AvrLm4-7* expression during *in vitro* growth and plant colonization of the compatible *Brassica napus* line Darmor-Bzh. Light grey bars are *AvrLm3* expression data from the A3a7 isolate G06-E107, that is displaying a virulent phenotype towards *Rlm7* and an avirulent phenotype towards *Rlm3*, medium grey bars, Nz-T4 isolate (a3a7 phenotype) and dark grey bars, v23.1.3 isolate (a3A7 phenotype). Black bars, *AvrLm4-7* expression for v23.1.3. Gene expression was assessed by qRT-PCR (quantitative reverse transcription-PCR). Expression levels were measured relatively to actin and EF1- α was used as a control. Error bars represent + SD for two to three technical replicates from two biological replicates. dpi, d post inoculation.

virulence towards *Rlm3* in Nz-T4, devoid of a functional allele of *AvrLm4-7*, is due to sequence polymorphism in *AvrLm3*. In v23.1.3, showing an a3 phenotype, but no *AvrLm3* sequence polymorphism compared to G06-E107, *AvrLm3* has the same kinetics of expression as in the A3 isolate G06-E107 (Fig. 5). This observation is in agreement with RNAseq data at 7 dpi, showing a high level of *AvrLm3* expression both in the WT G06-E107 A3a7 isolate, and in the complemented isolate G06-E107 + *AvrLm4-7* (a3A7) (Table S5). Therefore, the presence of a functional allele of *AvrLm4-7* does not modify *AvrLm3* expression, strongly suggesting that the a3 phenotype does not result from a suppression of *AvrLm3* expression caused by the presence of *AvrLm4-7*.

Absence of physical interaction between the AvrLm3 and AvrLm4-7 proteins *in vitro*

Diploid yeast strains from the cross between Y187-*AvrLm3* and Y2HGold-*AvrLm4-7*, or between Y187-*AvrLm4-7* and Y2HGold-*AvrLm3* did not grow in selective media (Fig. S6). In addition, AvrLm3 was not found as a putative AvrLm4-7 interactor in the Yeast two-hybrid screen of a cDNA library originating from cotyledons infected with an A3a7 isolate. These data suggest that AvrLm3 and AvrLm4-7 proteins do not interact physically, and that the masking of AvrLm3 phenotype by AvrLm4-7 is not linked with the ability of AvrLm4-7 to form a heterodimer with AvrLm3.

Discussion

In this paper, we report on the identification and the cloning of *AvrLm3*, an avirulence gene of *Leptosphaeria maculans*. Similar to other avirulence genes cloned in *L. maculans* (Gout *et al.*, 2006; Fudal *et al.*, 2007; Parlange *et al.*, 2009; Balesdent *et al.*, 2013; Ghanbarnia *et al.*, 2014; Van de Wouw *et al.*, 2014), *AvrLm3* is surrounded by repeat induced point mutations (RIP)-degenerated transposable elements (TEs) and encodes for a cysteine-rich small secreted protein. *AvrLm3* is highly expressed at early infection stages and it has no recognizable homologues in other fungal species including the closely related species *Leptosphaeria biglobosa* and *Leptosphaeria maculans* sp. *lepidii* (Grandaubert *et al.*, 2014). Although showing all features common to avirulence genes and proteins of *L. maculans*, *AvrLm3* is present in numerous isolates as a functional avirulence gene but the presence of a functional allele of *AvrLm4-7* 'hides' the *Rlm3*-mediated recognition of *AvrLm3*. By contrast, inactivated alleles (or lack) of *AvrLm4-7* leads to re-emergence of the *AvrLm3* avirulence phenotype.

The first cloned avirulence genes of *L. maculans*, *AvrLm1*, *AvrLm6* and *AvrLm4-7*, were identified by map-based cloning strategies (Gout *et al.*, 2006; Fudal *et al.*, 2007; Parlange *et al.*, 2009). Based on common characteristics of *L. maculans* avirulence genes, the whole genome sequence was the source of a repertoire of effector genes that were primary candidates in map-based cloning strategies of Avr genes. This allowed the rapid cloning of *AvrLm11*, in spite of its location on a dispensable

chromosome, which prevented any fine mapping in crosses involving virulent isolates missing the whole dispensable chromosome (Balesdent *et al.*, 2013). However, the location in large AT (adenine and thymine) isochores impedes in some cases the identification of a gene via map-based cloning. This was illustrated by the recent cloning of *AvrLm2* which was not immediately confused with the previously identified candidate effector *LmCys1* following a wrong map position resulting from contig misassemblies and gene conversion events. *AvrLm2* could only be unambiguously cloned by combining genetic mapping with NGS resequencing of multiple isolates to identify SNPs coincident with the virulent/avirulent phenotypes (Ghanbarnia *et al.*, 2014).

Cloning of *AvrLm3* combined additional levels of difficulties. First, the masking effect of *AvrLm4-7* on the *AvrLm3* phenotype complicated the gene mapping. Balesdent *et al.* (2002) reported a full co-segregation between the two genes, whereas a genetic distance of 14.9 cM was found here. Indeed the crosses studied in Balesdent *et al.* (2002) were also polymorphic for *AvrLm4-7* and progeny phenotyping for *AvrLm3* only revealed the segregation of *AvrLm4-7*, whose presence or absence hid, or not, the *Rlm3-AvrLm3* recognition. Here, a cross was set up between two isolates virulent towards *Rlm7* which allowed us to phenotype the *AvrLm3-Rlm3* interaction without any interference due to the presence of *AvrLm4-7*. Genetic mapping, the use of the repertoire of candidate effector genes, and mapping of RNA-seq reads on the reference genome allowed us neither to identify any candidate, nor to border the genetic interval on its 3' side. Moreover, the 3' end of the SC12 of the reference sequence, where *AvrLm3* is located, comprised unresolved gaps. Bacteria artificial chromosome (BAC) clones screening with markers of the genetic map, NGS sequencing of BAC clones and mapping RNA-seq reads on the BAC contigs were necessary to identify *AvrLm3*, located in a gap in the reference genome. The presence of telomere-specific repeats such as *LmTelo2* (Rouxel *et al.*, 2011) at both sides of the last gap of SC12 and in the BAC clones containing *AvrLm3* suggests that *AvrLm3* is located in a telomeric region.

We functionally validated the negative interaction occurring between AvrLm3 and AvrLm4-7 phenotypes, the *Rlm3*-mediated resistance being 'hidden' by the presence of a functional allele of *AvrLm4-7*. This is a new illustration of the complex arms race in progress during the co-evolution of plant and pathogens. Houterman *et al.* (2008) demonstrated that the *Avr1* Avr gene of *Fusarium oxysporum*, inducing *I-1* triggered resistance, also suppresses the protective effect of two other tomato resistance genes, *I-2* (when faced to *Avr2* isolates) and *I-3* (when faced to *Avr3* isolates). Recently, a similar mechanism has been described in the necrotrophic fungus *Pyrenophora tritici repentis*, where the Host Selective Toxin (HST) ToxA could suppress the activity of other HSTs, which still have to be characterized (Manning & Ciuffetti, 2015). Compared to these two examples, the effect of AvrLm4-7 on the *Rlm3-AvrLm3* recognition seems to be more specific because the presence of *AvrLm4-7* does not prevent expression of other avirulence phenotypes such as those due to *AvrLm1*, *AvrLm5* or *AvrLm6* (Balesdent *et al.*, 2006).

In *F. oxysporum*, no evidence of direct interaction has been found between Avr1, Avr2 and Avr3 avirulence proteins, and the mechanism of interference has remained unexplained since its description (Houterman *et al.*, 2008). Similarly, we could not find evidence of direct interaction between AvrLm3 and AvrLm4-7 using *in vitro* Y2H approaches. Several hypotheses could be proposed to explain the exclusion between avirulence phenotypes. First, the *Rlm3*-mediated resistance could be specifically suppressed by AvrLm4-7 as proposed by Houterman *et al.* (2008) for Avr1 being a potential suppressor of *I-2* and *I-3*-based immunity. That mechanism also occurs in the phytopathogenic bacteria *Xanthomonas campestris* pv. *vesicatoria* (Szczesny *et al.*, 2010). The avirulence protein AvrBsT interacts in the plant cell cytosol with SnRK1, an ABC transporter and a sucrose nonfermenting 1 (SNF1)-related kinase 1 to inhibit the HR induced by AvrBs1 recognition. In the *AvrLm3-AvrLm4-7* model, we found an earlier and higher level of *in planta* expression for *AvrLm3* compared to *AvrLm4-7*, a result that does not support a role for AvrLm4-7 activity in suppression of plant defence responses. However, the correlation between transcript and protein abundance is only partial and can be modulated by regulatory processes such as mRNA and protein degradation, or post-transcriptional modifications (Vogel & Marcotte, 2012).

Another hypothesis would imply that AvrLm3 and AvrLm4-7 have the same plant target, in the frame of a direct or a 'guard model' of interaction. In the fungus *Magnaporthe oryzae*, the two avirulence proteins Avr1-CO39 and Avr-Pia both target the pair of resistance proteins RGA4 and RGA5 to trigger Effector-Triggered-Immunity (ETI) (Cesari *et al.*, 2013). However, none of these two avirulence proteins has the ability to suppress the recognition of the other one. In *Pseudomonas syringae*, the effector proteins AvrRpm1, AvrRpt2, AvrB, AvrPto and HopF2 all target the *Arabidopsis thaliana* protein RIN4, a key regulator of plant immunity (Mackey *et al.*, 2002; Axtell & Staskawicz, 2003; Wilton *et al.*, 2010; Deslandes & Rivas, 2012). AvrB and AvrRPM1 trigger the RPM1-mediated resistance by phosphorylating RIN4. AvrRpt2-triggered immunity results from the cleavage of RIN4 by AvrRpt2, which therefore prevents the RPM1-mediated resistance. Finally, the effector protein HopF2 interferes with AvrRpt2 induced ETI. Future investigations of AvrLm3 and AvrLm4-7 plant targets and signalling pathways activated by both *Rlm3* and *Rlm7*-mediated resistance are needed to better understand mechanisms underlying that complex gene-for-gene interaction.

The location of *AvrLm3* in a telomeric region is consistent with the assumption that *L. maculans* effectors are located within RIP-affected AT-rich isochores (Rouxel *et al.*, 2011) but such a telomeric location has not been reported yet for *L. maculans* avirulence genes. Telomeres are often enriched in genes involved in niche adaptation in eukaryotes (Farman, 2007). For instance, many avirulence genes, including *AVR-Pii* and *AVR-Pita*, have been found in telomeric regions in *M. oryzae*, and loss of chromosome tips is suggested to be one frequent mechanism for gain of virulence (Orbach *et al.*, 2000; Farman, 2007; Yoshida *et al.*, 2009). In *L. maculans*, avirulence genes located in AT-rich regions generally evolve by complete deletions when submitted to

the resistance gene selection (Gout *et al.*, 2007) and one could expect an even greater instability due to its location within a telomeric AT isochore. Maintenance of *AvrLm3* in populations, as demonstrated here through the resurgence of the *AvrLm3* phenotype following *Rlm7* selection pressure, in spite of its telomeric location could indicate that *AvrLm3* plays an important role in the life cycle of the fungus. Such a fitness penalty is known for *Avr3* and *Avr2* of *F. oxysporum*, escaping to their recognition by resistance genes *I-3* and *I-2* through acquisition of *Avr1*, which suppresses the *Avr2* and *Avr3* triggered immunity, and not through loss of *Avr3* (Houterman *et al.*, 2008, 2009). As discussed by Houterman *et al.* (2008), such a complex interplay may lead to initially unpredicted strategies for disease control. Until now, the use of specific R genes to control *L. maculans* has resulted in very rapid breakdown of these resistances, as shown for *Rlm1*, *Rlm6* or the *B. rapa* resistance source *RlmS* (Sprague *et al.*, 2006). The fact that the breakdown of *Rlm7* gives birth to A3 isolates provides us with an unprecedented template with which to evaluate, using field experiments and modelling approaches, different strategies to increase the durability of a major resistance gene in these cases of complex gene-for-gene interactions.

Acknowledgements

The authors wish to thank Laurent Coudard (INRA BIOGER) for his major contribution to management of isolate collection, Bertrand Auclair (INRA BIOGER) for plant management, Régine Delourme (INRA, UMR IGEPP) for *B. napus* Darmorbzh seeds. This work was funded by the CTPS Project 'ICOSCOP', the INRA-SMaCH Metaprogram 'K-Masstec' and a grant from the Santé des Plantes et Environnement (SPE) INRA Department. G.D. was funded by the French Ministère de la Recherche et de l'Enseignement Supérieur and C.P. by a young scientist grant (Contrat Jeune Scientifique) from INRA.

Author contributions

C.P., T.R. and M-H.B. planned and designed the research. C.P., G.D., B.O., F.B., A.D., I.F., T.R. and M-H.B. performed the experiments. C.P., G.D., A.D., T.R. and M-H.B. analysed data. C.P., G.D., M-H.B. and T.R. drafted the manuscript, which was reviewed and revised by all authors.

References

- Ansan-Melayah D, Balesdent MH, Buée M, Rouxel T. 1995. Genetic characterization of *AvrLm1*, the first avirulence gene of *Leptosphaeria maculans*. *Phytopathology* 85: 1525–1529.
- Attard A, Gout L, Gourgues M, Kühn ML, Schmit J, Laroche S, Ansan-Melayah D, Billault A, Cattolico L, Balesdent MH *et al.* 2002. Analysis of molecular markers genetically linked to the *Leptosphaeria maculans* avirulence gene *AvrLm1* in field populations indicates a highly conserved event leading to virulence on *Rlm1* genotypes. *Molecular Plant–Microbe Interactions* 15: 672–682.
- Axtell MJ, Staskawicz BJ. 2003. Initiation of *RPS2*-specified disease resistance in *Arabidopsis* is coupled to the AvrRpt2-directed elimination of RIN4. *Cell* 112: 369–377.

- Balesdent MH, Attard A, Ansan-Melayah D, Delourme R, Renard M, Rouxel T. 2001. Genetic control and host range of avirulence toward *Brassica napus* cultivars Quinta and Jet Neuf in *Leptosphaeria maculans*. *Phytopathology* 91: 70–76.
- Balesdent MH, Attard A, Kühn ML, Rouxel T. 2002. New avirulence genes in the phytopathogenic fungus *Leptosphaeria maculans*. *Phytopathology* 92: 1122–1133.
- Balesdent MH, Barbetti M, Li Hua, Sivasithamparam K, Gout L, Rouxel T. 2005. Analysis of *Leptosphaeria maculans* race structure in a worldwide collection of isolates. *Phytopathology* 95: 1061–1071.
- Balesdent MH, Fudal I, Ollivier B, Bally P, Grandaubert J, Eber F, Chèvre AM, Leflon M, Rouxel T. 2013. The dispensable chromosome of *Leptosphaeria maculans* shelters an effector gene conferring avirulence towards *Brassica rapa*. *New Phytologist* 198: 887–898.
- Balesdent MH, Louvard K, Pinochet X, Rouxel T. 2006. A large-scale survey of races of *Leptosphaeria maculans* occurring on oilseed rape in France. *European Journal of Plant Pathology* 114: 53–65.
- Bally P, Grandaubert J, Rouxel T, Balesdent MH. 2010. FONZIE: an optimized pipeline for minisatellite marker discovery and primer design from large sequence data sets. *BMC Research Notes* 3: 322.
- Catanzariti A, Jones DA. 2010. Effector proteins of extracellular fungal plant pathogens that trigger host resistance. *Functional Plant Biology* 37: 901–906.
- Cesari S, Thilliez G, Ribot C, Chalvon V, Michel C, Jauneau A, Rivas S, Alaux L, Kanzaki H, Okuyama Y *et al.* 2013. The rice resistance protein pair RGA4/RGA5 recognizes the *Magnaporthe oryzae* effectors AVR-Pia and AVR1-CO39 by direct binding. *The Plant Cell* 25: 1463–1481.
- Chalhoub B, Denoed F, Liu S, Parkin IAP, Tang H, Wang X, Chiquet J, Belcram H, Tong C, Samans B *et al.* 2014. Early allopolyploid evolution in the post-Neolithic *Brassica napus* oilseed genome. *Science* 345: 950–953.
- Daverdin G, Rouxel T, Gout L, Aubertot JN, Fudal I, Meyer M, Parlange F, Carpezat J, Balesdent MH. 2012. Genome structure and reproductive behaviour influence the evolutionary potential of a fungal phytopathogen. *PLoS Pathogens* 8: e1003020.
- Delourme R, Chèvre AM, Brun H, Rouxel T, Balesdent MH, Dias J, Salisbury P, Renard M, Rimmer SR. 2006. Major gene and polygenic resistance to *Leptosphaeria maculans* in oilseed rape (*Brassica napus*). *European Journal of Plant Pathology* 114: 41–52.
- Deslandes L, Rivas S. 2012. Catch me if you can: bacterial effectors and plant targets. *Trends in Plant Science* 17: 644–655.
- Dilmaghani A, Balesdent MH, Didier JP, Wu C, Davey J, Barbetti MJ, Hua Li, Moreno-Rico O, Phillips D, Despeghel JP *et al.* 2009. The *Leptosphaeria maculans*–*Leptosphaeria biglobosa* species complex in the American continent. *Plant Pathology* 58: 1044–1058.
- Farman ML. 2007. Telomeres in the rice blast fungus *Magnaporthe oryzae*: the world of the end as we know it. *FEMS Microbiology Letters* 273: 125–132.
- Fudal I, Ross S, Gout L, Blaise F, Kuhn ML, Eckert MR, Cattolico L, Bernard-Samain S, Balesdent MH, Rouxel T. 2007. Heterochromatin-like regions as ecological niches for avirulence genes in the *Leptosphaeria maculans* genome: map-based cloning of *AvrLm6*. *Molecular Plant–Microbe Interactions* 20: 459–470.
- Galagan JE, Selker EU. 2004. RIP: the evolutionary cost of genome defense. *Trends in Genetics* 20: 417–423.
- Gall C, Balesdent MH, Robin P, Rouxel T. 1994. Tetrad analysis of acid phosphatase, soluble protein patterns and mating type in *Leptosphaeria maculans*. *Phytopathology* 84: 1299–1305.
- Ghanbarnia K, Fudal I, Larkan NJ, Links MG, Balesdent MH, Profotova B, Fernando WGD, Rouxel T, Borhan MH. 2014. Rapid identification of the *Leptosphaeria maculans* avirulence gene *AvrLm2*, using an intraspecific comparative genomics approach. *Molecular Plant Pathology* 16: 699–709.
- Ghanbarnia K, Lydiate DJ, Rimmer SR, Li G, Kutcher HR, Larkan NJ, McVetty PBE, Fernando WGD. 2012. Genetic mapping of the *Leptosphaeria maculans* avirulence gene corresponding to the *LepRI* resistance gene of *Brassica napus*. *Theoretical and Applied Genetics* 124: 505–513.
- Gout L, Fudal I, Kuhn ML, Blaise F, Eckert M, Cattolico L, Balesdent MH, Rouxel T. 2006. Lost in the middle of nowhere: the *AvrLm1* avirulence gene of the Dothideomycete *Leptosphaeria maculans*. *Molecular Microbiology* 60: 67–80.
- Gout L, Kuhn ML, Vincenot L, Bernard-Samain S, Cattolico L, Barbetti M, Moreno-Rico O, Balesdent MH, Rouxel T. 2007. Genome structure impacts molecular evolution at the *AvrLm1* avirulence locus of the plant pathogen *Leptosphaeria maculans*. *Environmental Microbiology* 9: 2978–2992.
- Grandaubert J, Lowe RG, Soyer JL, Schoch CL, Van de Wouw AP, Fudal I, Robbertse B, Lapalu N, Links MG, Ollivier B *et al.* 2014. Transposable element-assisted evolution and adaptation to host plant within the *Leptosphaeria maculans*–*Leptosphaeria biglobosa* species complex of fungal pathogens. *BMC Genomics* 15: 891.
- Houterman PM, Cornelissen BJC, Rep M. 2008. Suppression of plant resistance gene-based immunity by a fungal effector. *PLoS Pathogens* 4: e1000061.
- Houterman PM, Ma L, Van Ooijen G, De Vroomen MJ, Cornelissen BJC, Takken FLW, Rep M. 2009. The effector protein Avr2 of the xylem-colonizing fungus *Fusarium oxysporum* activates the tomato resistance protein I-2 intracellularly. *Plant Journal* 58: 970–978.
- de Jonge R, Bolton MD, Thomma BP. 2011. How filamentous pathogens co-opt plants: the ins and outs of fungal effectors. *Current Opinion in Plant Biology* 14: 400–406.
- Koeck M, Hardham AR, Dodds PN. 2011. The role of effectors of biotrophic and hemibiotrophic fungi in infection. *Cellular Microbiology* 13: 1849–1857.
- Livak KJ, Schmittgen TD. 2001. Analysis of relative gene expression data using real-time quantitative PCR and the $2^{-\Delta\Delta C_t}$ method. *Methods* 25: 402–408.
- Mackey D, Holt BF, Wiig A, Dangl JL. 2002. RIN4 interacts with *Pseudomonas syringae* type III effector molecules and is required for *RPM1*-mediated resistance in *Arabidopsis*. *Cell* 108: 743–754.
- Manning VA, Ciuffetti LM. 2015. Necrotrophic effector epistasis in the *Pyrenophora tritici-repentis*–wheat interaction. *PLoS ONE* 10: e0123548.
- McDonald BA, Linde C. 2002. Pathogen population genetics, evolutionary potential, and durable resistance. *Annual Review of Phytopathology* 40: 349–379.
- Muller PY, Janovjak H, Miserez AR, Dobbie Z. 2002. Processing of gene expression data generated by quantitative real-time RT-PCR. *BioTechniques* 32: 1372–1379.
- Orbach MJ, Farrall L, Sweigard JA, Chumley FG, Valent B. 2000. A telomeric avirulence gene determines efficacy for the rice blast resistance gene *Pi-ta*. *The Plant Cell* 12: 2019–2032.
- Parlange F, Daverdin G, Fudal I, Kuhn ML, Balesdent MH, Blaise F, Grezes-Beset B, Rouxel T. 2009. *Leptosphaeria maculans* avirulence gene *AvrLm4-7* confers a dual recognition specificity by the *Rlm4* and *Rlm7* resistance genes of oilseed rape, and circumvents *Rlm4*-mediated recognition through a single amino acid change. *Molecular Microbiology* 71: 851–863.
- Petersen TN, Brunak S, von Heijne G, Nielsen H. 2011. SignalP 4.0: discriminating signal peptides from transmembrane regions. *Nature Methods* 8: 785–786.
- Rouxel T, Grandaubert J, Hane JK, Hoede C, van de Wouw AP, Couloux A, Dominguez V, Anthouard V, Bally P, Bourras S *et al.* 2011. Effector diversification within compartments of the *Leptosphaeria maculans* genome affected by Repeat-Induced Point mutations. *Nature Communications* 2: 202.
- Rozen S, Skaletsky H. 2000. Primer3 on the www for general users and for biologist programmers. *Methods in Molecular Biology* 132: 365–386.
- Sprague SJ, Balesdent MH, Brun H, Hayden HL, Marcroft SJ, Pinochet X, Rouxel T, Howlett BJ. 2006. Major gene resistance in *Brassica napus* (oilseed rape) is overcome by changes in virulence of populations of *Leptosphaeria maculans* in France and Australia. *European Journal of Plant Pathology* 114: 33–40.
- Szczesny R, Büttner D, Escolar J, Schulze S, Seiferth A, Bonas U. 2010. Suppression of the *AvrBs1*-specific hypersensitive response by the YopJ effector homolog AvrBsT from *Xanthomonas* depends on a SNF1-related kinase. *New Phytologist* 187: 1058–1074.
- Van de Wouw AP, Lowe RGT, Elliott CE, Dubois DJ, Howlett BJ. 2014. An avirulence gene, *AvrLmJ1*, from the blackleg fungus, *Leptosphaeria maculans*, confers avirulence to *Brassica juncea* cultivars. *Molecular Plant Pathology* 15: 523–530.
- Vogel C, Marcotte EM. 2012. Insights into the regulation of protein abundance from proteomic and transcriptomic analyses. *Nature Reviews Genetics* 13: 227–232.
- Wilton M, Subramaniam R, Elmore J, Felsensteiner C, Coaker G, Desveaux D. 2010. The type III effector HopF2_{Pto} targets *Arabidopsis* RIN4 protein to

promote *Pseudomonas syringae* virulence. *Proceedings of the National Academy of Sciences, USA* 107: 2349–2354.

Wu L, Chen H, Curtis C, Fu ZQ. 2014. Go in for the kill: how plants deploy effector-triggered immunity to combat pathogens. *Virulence* 5: 710–721.

Yoshida K, Saitoh H, Fujisawa S, Kanzaki H, Matsumura H, Yoshida K, Tosa Y, Chuma I, Takano Y, Win J *et al.* 2009. Association genetics reveals three novel avirulence genes from the rice blast fungal pathogen *Magnaporthe oryzae*. *The Plant Cell Online* 21: 1573–1591.

Supporting Information

Additional supporting information may be found in the online version of this article.

Fig. S1 Interaction phenotype of wild-type and transformed *Leptosphaeria maculans* isolates on *Rlm3* and *Rlm7* lines.

Fig. S2 Characterization of *Leptosphaeria maculans* isolates silenced for *AvrLm4-7*.

Fig. S3 Genetic mapping and relative expression of *AvrLm3* using HRM method.

Fig. S4 Sequence alignment between the avirulence proteins *AvrLm3* and *AvrLmJ1* of *Leptosphaeria maculans*.

Fig. S5 Functional validation of *AvrLm3* by silencing experiments.

Fig. S6 Absence of physical interaction between *AvrLm3* and *AvrLm4-7* proteins in a yeast-two-hybrid heterologous system.

Table S1 List and characteristics of the oilseed rape (*Brassica napus*) lines used

Table S2 List and characteristics of polymorphic molecular markers used for *AvrLm3* mapping in cross no. 69

Table S3 Primers used for vector constructions and qRT-PCR

Table S4 List of transformation experiments of *Leptosphaeria maculans* isolates

Table S5 Top 25 genes expressed by four *L. maculans* isolates at 7 d post inoculation of the compatible *Brassica napus* cultivar Darmor-bzh

Table S6 *AvrLm3* sequence polymorphism between G06-E107 and Nz-T4, the parent isolates of cross no. 69

Please note: Wiley Blackwell are not responsible for the content or functionality of any supporting information supplied by the authors. Any queries (other than missing material) should be directed to the *New Phytologist* Central Office.



About New Phytologist

- *New Phytologist* is an electronic (online-only) journal owned by the New Phytologist Trust, a **not-for-profit organization** dedicated to the promotion of plant science, facilitating projects from symposia to free access for our Tansley reviews.
- Regular papers, Letters, Research reviews, Rapid reports and both Modelling/Theory and Methods papers are encouraged. We are committed to rapid processing, from online submission through to publication 'as ready' via *Early View* – our average time to decision is <27 days. There are **no page or colour charges** and a PDF version will be provided for each article.
- The journal is available online at Wiley Online Library. Visit **www.newphytologist.com** to search the articles and register for table of contents email alerts.
- If you have any questions, do get in touch with Central Office (np-centraloffice@lancaster.ac.uk) or, if it is more convenient, our USA Office (np-usaoffice@lancaster.ac.uk)
- For submission instructions, subscription and all the latest information visit **www.newphytologist.com**